

Modeling and Control Simulation for a Condensate Distillation Column

Vu Trieu Minh and John Pumwa
*Papua New Guinea University of Technology (UNITECH), Lae
Papua New Guinea*

1. Introduction

Distillation is a process that separates two or more components into an overhead distillate and a bottoms product. The bottoms product is almost exclusively liquid, while the distillate may be liquid or a vapor or both.

The separation process requires three things. Firstly, a second phase must be formed so that both liquid and vapor phases are present and can contact each other on each stage within a separation column. Secondly, the components have different volatilities so that they will partition between the two phases to a different extent. Lastly, the two phases can be separated by gravity or other mechanical means.

Calculation of the distillation column in this chapter is based on a real petroleum project to build a gas processing plant to raise the utility value of condensate. The nominal capacity of the plant is 130,000 tons of raw condensate per year based on 24 operating hours per day and 350 working days per year. The quality of the output products is the purity of the distillate, x_D , higher than or equal to 98% and the impurity of the bottoms, x_B , may be less/equal than 2%. The basic feed stock data and its actual compositions are based on the other literature (PetroVietnam Gas Company, 1999).

The distillation column contains one feed component, x_F . The product stream exiting the top has a composition of x_D of the light component. The product stream leaving the bottom contains a composition of x_B of the light component. The column is broken in two sections. The top section is referred to as the rectifying section. The bottom section is known as the stripping section as shown in Figure 1.1.

The top product stream passes through a total condenser. This effectively condenses all of the vapor distillate to liquid. The bottom product stream uses a partial re-boiler. This allows for the input of energy into the column. Distillation of condensate (or natural gasoline) is cutting off light components as propane and butane to ensure the saturated vapor pressure and volatility of the final product.

The goals of this chapter are twofold: first, to present a theoretical calculation procedure of a condensate column for simulation and analysis as an initial step of a project feasibility study, and second, for the controller design: a reduced-order linear model is derived such that it best reflects the dynamics of the distillation process and used as the reference model

- b. *Fractionation*: Increasing the reflux ratio (or boil-up rate) will reduce the impurities in both distillate and the bottoms product.

Feed split usually has a much stronger effect on product compositions than does fractionation. One of the important consequences of the overwhelming effect of feed split is that it is usually impossible to control any composition (or temperature) in a column if the feed split is fixed (i.e. the distillate or the bottoms product flows are held constant). Any small changes in feed rate or feed composition will drastically affect the compositions of both products, and will not be possible to change fractionation enough to counter this effect.

2.1.2 Degrees of freedom of the distillation process

The degrees of freedom of a process system are the independent variables that must be specified in order to define the process completely. Consequently, the desired control of a process will be achieved when and only when all degrees of freedom have been specified. The mathematical approach to determine the degrees of freedom of any process (George, S., 1986) is to sum up all the variables and subtract the number of independent equations. However, there is a much easier approach developed by Waller, V. (1992): There are five control valves as shown in Figure 1.2, one on each of the following streams: distillate, reflux, coolant, bottoms and heating medium. The feed stream is considered being set by the upstream process. So this column has five degrees of freedom. Inventories in any process must be always controlled. Inventory loops involve liquid levels and pressures. This means that the liquid level in the reflux drum, the liquid level in the column base, and the column pressure must be controlled.

If we subtract the three variables that must be controlled from five, we end up with two degrees of freedom. Thus, there are two and only two additional variables that can (and must) be controlled in the distillation column. Notice that we have made no assumptions about the number or type of chemical components being distilled. Therefore a simple, ideal, binary system has two degrees of freedom; a complex, multi-component system also has two degrees of freedom.

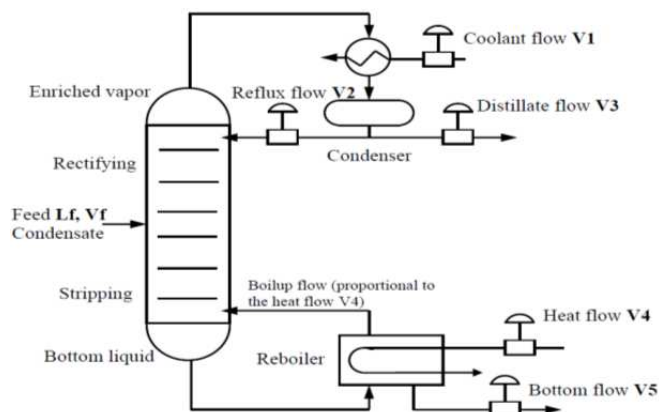


Fig. 2.1. Control Valves Location

2.1.3 Control structure

The manipulated variables and controlled variables of a distillation column are displayed in the Table 2.1 and in the Figure 2.1.

	Controlled variables	Manipulated variables	Control valve
1	Column pressure	Condenser duty	Coolant flow V1
2	Concentration (temperature) of distillate	Reflux flow rate	Reflux flow V2
3	Liquid level in the reflux drum	Distillate flow rate	Distillate flow V3
4	Concentration (temperature) of bottoms	Re-boiler duty	Heat flow V4
5	Liquid level in the column base	Bottoms flow rate	Bottom flow V5

Table 2.1. Manipulated variables and controlled variables of a distillation column

Selecting a control structure is a complex problem with many facets. It requires looking at the column control problem from several perspectives:

- Local perspective considering the steady state characteristics of the column.
- Local perspective considering the dynamic characteristics of the column.
- Global perspective considering the interaction of the column with other unit operations in the plant.

2.1.4 Energy balance control structure (L-V)

The *L-V* control structure, which is called energy balance structure, can be viewed as the *standard control structure* for dual composition control of distillation. In this control structure, the reflux flow rate *L* and the boil-up flow rate *V* are used to control the “primary” outputs associated with the product specifications. The liquid holdups in the drum and in the column base (the “secondary” outputs) are usually controlled by distillate flow rate *D* and the bottoms flow rate *B*.

2.1.5 Material balance control structure (D-V) and (L-B)

Two other frequently used control structures are the material balance structures (*D-V*) and (*L-B*). The (*D-V*) structure seems very similar to the (*L-V*) structure. The only difference between the (*L-V*) and the (*D-V*) structures is that the roles of *L* and *D* are switched.

2.2 Distillation process calculation

2.2.1 Preparation for initial data

The plant nominal capacity is 130,000 tons of raw condensate per year based on 24 operating hours per day and 350 working days per year. The plant equipment is specified with a design margin of 10% above the nominal capacity and turndown ratio of 50%. Hence, the raw condensate *feed rate* for the plant is determined as follows:

$$Feed = \frac{130,000 \text{ tons}}{(24 \text{ h}) \times (350 \text{ working days})} = 15.47619 \text{ tons / hour} \quad (2.1)$$

The actual composition of the raw condensate for the gas processing plant is always fluctuates around the average composition as shown in the Table 2.2. The distillation data for given raw condensate are shown in the Table 2.3.

Component	Mole %
Propane	0.00
Normal Butane	19.00
Iso-butane	26.65
Iso-pentane	20.95
Normal Pentane	10.05
Hexane	7.26
Heptane	3.23
Octane	1.21
Nonane	0.00
Normal Decane	0.00
n-C11H24	1.94
n-C12H26	2.02
Cyclopentane	1.61
Methylclopentane	2.02
Benzene	1.61
Toluen	0.00
O-xylene	0.00
E-benzen	0.00
124-Mbenzen	0.00

Table 2.2. Compositions of raw condensate

The feed is considered as a pseudo *binary mixture* of Ligas (iso-butane, n-butane and propane) and Naphthas (iso-pentane, n-pentane, and heavier components). The column is designed with $N=14$ trays. The model is simplified by lumping some components together (pseudocomponents) and modeling of the column dynamics is based on these pseudocomponents only (Kehlen, H. & Ratzsch, M., 1987). Depending on the feed composition fluctuation, the properties of pseudo components are allowed to change within the range as shown in the Table 2.4.

Relative volatility:

Relative volatility is a measure of the differences in volatility between two components, and hence their boiling points. It indicates how easy or difficult a particular separation will be. The relative volatility of component i with respect to component j is defined as:

$$\alpha_{ij} = \frac{\left[\frac{y_i}{x_i} \right]}{\left[\frac{y_j}{x_j} \right]} = \frac{K_i}{K_j} \quad \text{where} \quad \begin{cases} y_i = \text{mole fraction of component } i \text{ in the vapor} \\ x_i = \text{mole fraction of component } i \text{ in the liquid} \end{cases}$$

Cut point (%)	Testing methods	
	TBP (°C)	ASTM (°C)
0.00	-1.44	31.22
1.00	-0.80	31.63
2.00	1.61	32.94
3.50	6.09	35.33
5.00	10.56	37.72
7.50	18.02	40.29
10.00	24.67	45.29
12.50	28.56	47.32
15.00	29.57	47.84
17.50	30.57	48.35
20.00	31.58	48.86
25.00	33.59	49.89
30.00	35.99	51.09
35.00	39.12	52.92
40.00	43.94	55.83
45.00	50.00	59.64
50.00	58.42	65.19
55.00	66.23	70.38
60.00	69.51	72.55
65.00	70.77	73.34
70.00	75.91	76.68
75.00	86.06	84.11
80.00	98.63	94.20
85.00	100.57	95.91
90.00	115.54	109.54
92.50	125.47	118.90
95.00	131.07	124.24
96.50	138.36	131.05
98.00	148.30	140.20
99.00	159.91	146.78
100.00	168.02	156.75

Table 2.3. Distillation data

Properties	Ligas	Naphthas
Molar weight	54.4-55.6	84.1-86.3
Liquid density (kg/m ³)	570-575	725-735
Feed composition (vol %)	38-42	58-62

Table 2.4. Properties of the pseudo components

Checking the data in the handbook (Perry, R. & Green, D., 1984) for the operating range of temperature and pressure, the relative volatility is calculated as: $\alpha = 5.68$.

Correlation between TBP and Equilibrium Flash Vaporization (EFV):

The EFV curve is converted from the TBP data according to (Luyben, W., 1990). The initial data are:

$$t_{50\%(TBP)} = 58.42 \text{ } ^\circ\text{C}$$

$$t_{(30\%-10\%)(TBP)} = 35.99 - 24.67 = 11.32 \text{ } ^\circ\text{C}$$

Consulting TBP-EFV correlation chart, we obtain $t_{50\%(EFV-TBP)} = 5.2 \text{ } ^\circ\text{C}$

Therefore: $t_{50\%(EFV)} = 58.42 + 5.2 = 63.62 \text{ } ^\circ\text{C}$

Repeating the above procedure for all TBP data, the EFV (1 atm) data are determined. Then convert the EFV (1 atm) data into the EFV (4.6 atm) data by using Cox chart. The results are shown in the Table 2.5.

Operating pressure:

The column is designed with 14 trays, and the pressure drop across each tray is 80 kPa. Thus the pressures at feed section and top section are 4.6 atm and 4 atm respectively.

% vol.	TBP		EFV (1 atm)		EFV (4.6 atm)
	t °C	Δt	Δt	t °C	t °C
I.B.P.	-1.44			41.62	93
		1.2	1.5		
5	10.56			43.12	95
		14.11	4		
10	24.67			47.12	102
		6.91	3		
20	31.58			50.12	106
		4.41	2.5		
30	35.99			52.62	110
		7.95	5		
40	43.93			57.62	116
		14.48	6		
50	58.42			63.62	125
		11.09	5.5		
60	69.51			69.12	132
		6.4	6.5		
70	75.91			75.62	141
		22.72	7.5		
80	98.63			83.12	150
		16.91	7		
	115.54			90.12	158

Table 2.5. Correlation between TBP and EFV of raw condensate

2.2.2 Calculation for feed section

The feed is in liquid-gas equilibrium with gas percentage of 38% volume. However it is usual to deeply cut 4% of the unexpected heavy components, which will be condensed and refluxed to the column bottom. Thus there are two equilibrium phase flows: vapor $V_F=38+4=42\%$ and liquid $L_F=100-42=58\%$.

Operating temperature:

Consulting the EFV curve (4.6 atm) of feed section, the required feed temperature is 118 °C corresponding to 42% volume point.

The phase equilibrium is shown in the Figure 2.2.

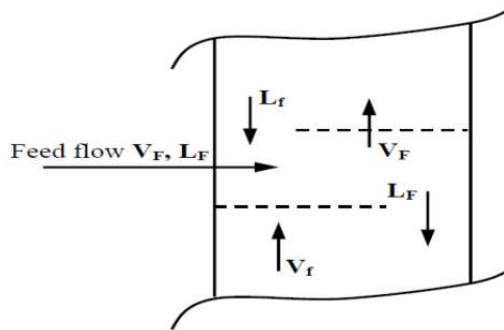


Fig. 2.2. The Equilibrium phase flows at the feed section

Where, V_F : Vapor phase rate in the feed flow; L_F : Liquid phase rate in the feed flow; V_f : Vapor flow arising from the stripping section; L_f : Internal reflux descending across the feed section.

The heavy fraction flow L_f dissolved an amount of light components is descending to the column bottom. These undesirable light components shall be caught by the vapor flow V_f arising to the top column. V_f , which can be calculated by empirical method, is equal to 28% vol. The bottoms product flow B is determined by yield curve as 62% vol. Hence, the internal reflux across the feed section can be computed as: $L_f = B - L_F + V_f = 62 + 28 = 32\% \text{ vol}$.

Material balances for the feed section is shown in the Table 2.6. The calculation based on the raw condensate *feed rate* for the plant: 15.4762 tons/hour.

2.2.3 Calculation for stripping section

In the stripping section, liquid flows, which are descending from the feed section, include the equilibrium phase flow L_F , and the internal reflux flow L_f . They are contacting with the arising vapor flow V_f for heat transfer and mass transfer. This process is accomplished with the aid of heat flow supplied by the re-boiler.

Main parameters to be determined are the bottoms product temperature and the re-boiler duty Q_B .

Stream	Volume fraction % vol	Liquid flow rate m ³ /h	Liquid density ton/ m ³	Mass flow rate ton/h
V_F	42	10.9983	0.591	6.5000
V_f	28	7.2464	0.598	4.3333
L_f	-32	-8.0527	0.615	-4.9524
Total light fraction	38	10.1923	0.577	5.8810
L_F	58	12.3639	0.726	8.9762
V_f	-28	-7.2464	0.598	-4.3333
L_f	32	8.0527	0.615	4.9524
B	62	13.1984	0.727	9.5952

Table 2.6. Material Balances for the Feed Section

The column base pressure is approximately the pressure at the feed section because pressure drop across this section is negligible. Consulting the EFV curve of stripping section and the Cox chart, the equilibrium temperature at this section is 144 °C. The re-boiler duty is equal to heat input in order to generate boil-up of stripping section an increment of 144-118=26 °C.

The material and energy balances for stripping section is displayed in the Table 2.7 and with one $cal_{TC} = 4.184$ J.

⇒ The re-boiler duty must be supplied: $Q_B = 6283.535 - 3983.575 = 2299.96 * 10^3$ (kJ/h).

INLET				
	ton/h	kcal/kg	kcal/h.10 ³	kJ/h.10 ³
L_F	8.9762	68	610.3816	2553.837
L_f	4.9524	69	341.7156	1429.738
Total	13.9286		952.0972	3983.575
OUTLET				
	ton/h	kcal/kg	kcal/h.10 ³	kJ/h.10 ³
V_f	4.3333	165	714.9945	2991.537
B	9.5952	82	786.8064	3291.998
Total	13.9285		1501.801	6283.535

Table 2.7. Material and Energy Balances for Stripping Section

2.2.4 Calculation for rectifying section

The overhead vapor flow, which includes V_F from feed section and V_f from stripping section, passes through the condenser (to remove heat) and then enter into the reflux drum. There exists two equilibrium phases: liquid (butane as major amount) and vapor (butane vapor, uncondensed gas - dry gas: C_1 , C_2 , e.g.). The liquid from the reflux drum is partly pumped back into the top tray as reflux flow L and partly removed as distillate flow D . The top pressure is 4 atm due to pressure drop across the rectifying section. The dew point of distillate is correspondingly the point 100% of the EFV curve of rectifying section. Also consulting the Cox chart, the top section temperature is determined as 46 °C.

The equilibrium phase flows at the rectifying sections are displayed in the Table 2.8.

INLET				
	ton/h	kcal/kg	kcal/h.10 ³	kJ/h.10 ³
V_F+V_f	10.8333	115	1245.83	5212.553
L_0	L_0	24	$24 \times L_0$	$100.416 \times L_0$
Total	$10.8333 + L_0$		$1245.83 + 24 \times L_0$	$5212.553 + 100.416 \times L_0$
OUTLET				
	ton/h	kcal/kg	kcal/h.10 ³	kJ/h.10 ³
Total light fraction+ L_0	$5.8810 + L_0$	97	$570.457 + 97 \times L_0$	$2386.792 + 405.848 \times L_0$
L_f	4.9524	16	79.2384	331.533
Total	$10.8334 + L_0$		$649.695 + 97 \times L_0$	$2718.326 + 405.848 \times L_0$

Table 2.8. Material and Energy Balances for Rectifying Section

Calculate the internal reflux flow L_0 : Energy balance, INLET=OUTLET:

$$5212.553 + 100.416L_0 = 2718.326 + 405.848L_0 \Rightarrow L_0 = 8.166 \text{ (ton/h)}$$

$$\Rightarrow \text{Total light fraction} + L_0 = 14.047 \text{ (ton/h)}$$

Calculate the external reflux flow L : Enthalpy data of reflux flow L looked up the experimental chart for petroleum enthalpy are corresponding to the liquid state of 40 °C (liquid inlet at the top tray) and the vapor state of 46 °C (vapor outlet at the column top).

L inlet at 40 °C: $H_{\text{liquid(inlet)}} = 22 \text{ kcal/kg}$; L outlet at 46 °C: $H_{\text{vapor(outlet)}} = 106 \text{ kcal/kg}$. Then,

$$\Delta H_{L_0} \times L_0 = \Delta H_L \times L \Rightarrow (115 - 24)(8.166) = (106 - 22)L \Rightarrow L = 8.847 \text{ (ton/h)}.$$

2.2.5 Latent heat and boil-up flow rate

The heat input of Q_B (re-boiler duty) to the reboiler is to increase the temperature of stripping section and to generate boil-up V_0 as (Franks, R., 1972): $V_0 = \frac{Q_B - Bc_B(t_B - t_F)}{\lambda}$, where, Q_B : re-boiler duty - 2299.96*10³ (kJ/h); B : flow rate of bottom product - 9595.2 (kg/h); c_B : specific heat capacity - 85 (kJ/kg. °C); t_F : inlet temperature - 118 (°C, the feed temperature); t_B : outlet temperature - 144 °C; λ : the latent heat or heat of vaporization.

The latent heat at any temperature is described in terms of the latent heat at the normal boiling point (Nelson, W., 1985): $\lambda = \gamma \lambda_B \frac{T}{T_B}$ (kJ/kg), where, λ : latent heat at absolute temperature T (kJ/kg); λ_B : latent heat at absolute normal boiling point T_B (kJ/kg); γ : correction factor obtained from the empirical chart. The result: $\lambda = 8500$ (kJ/kg); $V_0 = 4540.42$ (kg/h) or 77.67 (kmole/h); $V_f = 4333.3$ (kg/h) or 74.13 (kmole/h). The average vapor flow rate is rising in the stripping section $V = \frac{V_0 + V_f}{2} = \frac{77.67 + 74.13}{2} = 75.9$ (kmole/h).

2.2.6 Liquid holdup

Major design parameters to determine the liquid holdup on a tray, column base and reflux drum are calculated mainly based on other literature (Joshi, M., 1979; Wanrren, L. *et al.*, 2005; & Wuithier, P., 1972):

Velocity of vapor phase arising in the column: $\omega_n = C \sqrt{\frac{\rho_L - \rho_G}{\rho_G}}$ (m/s), where: ρ_L : density of liquid phase; ρ_G : density of vapor phase; C : correction factor depending flow rates of two-phase flows, obtained from the empirical chart, $C_f - P_f$ with $P_f = \frac{L}{G} \sqrt{\frac{\rho_G}{\rho_L}}$. The actual velocity ω is normally selected that $\omega = (0.80 - 0.85)\omega_n$ for paraffinic vapor. The diameter of the column is calculated with the formula: $D_k = \sqrt{\frac{4V_m}{3600\pi\omega}}$ (m), where, V_m : the mean flow of vapor in the column. Result: $D_k = 1.75$ (m).

The height of the column is calculated on distance of trays. The distance is selected on basis of the column diameter. The holdup in the column base is determined as:

$$M_B = \frac{\pi H_{NB} D_k^2}{4} \frac{d_B}{(MW)_B} \quad (\text{kmole}) \quad (2.2)$$

where: H_{NB} : normal liquid level in the column base (m); $(MW)_B$: molar weight of the bottom product (kg/kmole); d_B : density of the bottom product (kg/m³). Then,

$$\Rightarrow M_B = \frac{3.14(1.4)(1.75)^2}{4} \frac{726.5}{78.6} = 31.11 \text{ (kmole)}.$$

The holdup on each tray: $M = \frac{0.95\pi h_T D_k^2}{4} \frac{d_T}{(MW)_T}$ (kmole), where, h_T : average depth of clear liquid on a tray (m); $(MW)_T$: molar weight of the liquid holdup on a tray (kg/kmole); d_T : the mean density of the liquid holdup on a tray (kg/m³). Then,

$$\Rightarrow M = \frac{0.95(3.14)(0.28)(1.75)^2}{4} \frac{680}{75} = 5.80 \text{ kmole}.$$

The holdup in the reflux drum: Liquid holdup M_D is equal to the quantity of distillate contained in the reflux drum, $M_D = \frac{5(L_f + D_f)}{60}$ (kmole), where, M_D : holdup in the reflux drum; L_f : the reflux flow rate - (4952.4 kg/h)/(60.1 mole weight) = 82.4 kmole/h; V_f : the distillate flow rate - (4333.3 kg/h)/(58.2 mole weight) = 74.46 kmole/h. Then, $\Rightarrow M_D = \frac{5(82.4 + 74.46)}{60} = 13.07$ (kmole).

3. Mathematic model

3.1 Equations for flows throughout general trays

The total mole holdup in the n^{th} tray M_n is considered constant, but the imbalance in the input and output flows is taken into account for in the component and heat balance equations as shown in Figure 3.1.

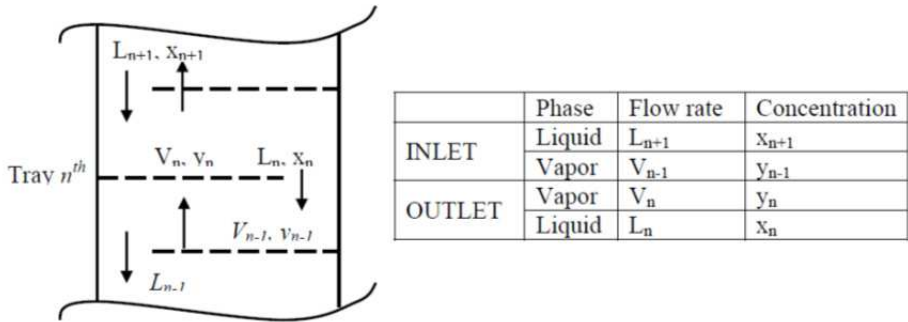


Fig. 3.1. A General n^{th} Tray

Total mass balance:

$$\frac{d(M_n)}{dt} = L_{n+1} - L_n + V_{n-1} - V_n \quad (3.1)$$

Component balance:

$$\frac{d(M_n x_n)}{dt} = L_{n+1} x_{n+1} - L_n x_n + V_{n-1} y_{n-1} - V_n y_n \quad (3.2)$$

By differentiating (3.2) and substituting for (3.1), the following expression is obtained:

$$\frac{d(x_n)}{dt} = \frac{L_{n+1} x_{n+1} + V_{n-1} y_{n-1} - (L_{n+1} + V_{n-1}) x_n - V_n (y_n - x_n)}{M_n} \quad (3.3)$$

Energy balance:

$$\frac{d(M_n h_n)}{dt} = h_{n+1} L_{n+1} - h_n L_n + H_{n-1} V_{n-1} - H_n V_n \quad (3.4)$$

or

$$M_n \frac{dh_n}{dt} + h_n \frac{dM_n}{dt} = h_{n+1} L_{n+1} + H_{n-1} V_{n-1} - h_n L_n - H_n V_n \quad (3.5)$$

Because the term $\frac{dh_n}{dt}$ is approximately zero, substituting for the change of hold up $\frac{dM_n}{dt}$ in (3.5), and rearranging the terms, the following expression is obtained:

$$V_n = \frac{h_{n+1}L_{n+1} + H_{n-1}V_{n-1} - (L_{n+1} + V_{n-1})h_n}{H_n - h_n} \tag{3.6}$$

where, n: tray n^{th} ; V: vapor flow; L: liquid flow; x: liquid concentration of light component; y: vapor concentration of light component; h: enthalpy for liquid; H: enthalpy for vapor.

3.2 Equations for the feed tray: (Stage n=f) (See Figure 3.2)

Total mass balance:

$$\frac{d(M_f)}{dt} = F + L_{f+1} + V_{f-1} - L_f - V_f \tag{3.7}$$

Component balance:

$$\begin{aligned} \frac{d(M_f x_f)}{dt} &= Fc_f + L_{f+1}x_{f+1} + V_{f-1}y_{f-1} - L_f x_f - V_f y_f \\ \Rightarrow \frac{dx_n}{dt} &= \frac{L_{n+1}x_{n+1} + V_{n-1}y_{n-1} - (L_{n+1} + V_{n-1})x_n - V_n(y_n - x_n)}{M_n} \end{aligned} \tag{3.8}$$

Energy balance:

$$\begin{aligned} \frac{d(M_f h_f)}{dt} &= h_f F + h_{n+1}L_{n+1} + H_{n-1}V_{n-1} - h_n L_n - H_n V_n \\ \Rightarrow V_n &= \frac{h_f F + h_{n+1}L_{n+1} + H_{n-1}V_{n-1} - (L_{n+1} + V_{n-1})h_n}{H_n - h_n} \end{aligned} \tag{3.9}$$

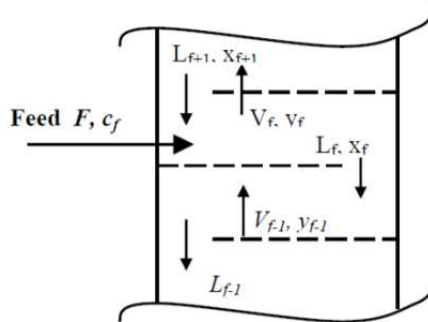


Fig. 3.2. Feed Section

3.3 Equations for the top section: (stage $n=N+1$) (See Figure 3.3)

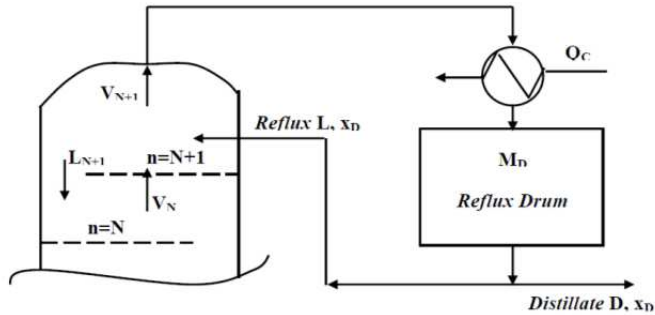


Fig. 3.3. Top Section and Reflux Drum

Equations for the top tray (stage $n=N+1$)

Total mass balance:

$$\frac{d(M_{N+1})}{dt} = L + V_N - L_{N+1} - V_{N+1} \quad (3.10)$$

Component balance:

$$\frac{d(M_{N+1}x_{N+1})}{dt} = Lx_D + V_Ny_N - L_{N+1}x_{N+1} - V_{N+1}y_{N+1} \quad (3.11)$$

Energy balance:

$$\frac{d(M_{N+1}h_{N+1})}{dt} = h_D L + H_N V_N - h_{N+1} L_{N+1} - H_{N+1} V_{N+1} \quad (3.12)$$

$$\Rightarrow V_{N+1} = \frac{h_D L + H_N V_N - (L + V_N)h_{N+1}}{H_{N+1} - h_{N+1}} \quad (3.13)$$

Reflux drum and condenser

Total mass balance:

$$\frac{d(M_D)}{dt} = V_{N+1} - L - D \quad (3.14)$$

Component balance:

$$\frac{d(M_D x_D)}{dt} = V_{N+1} y_{N+1} - (L + D) x_D \quad (3.15)$$

Energy balance around condenser:

The condenser duty Q_C is equal to the latent heat required to condense the overhead vapor to bubble point:

$$Q_C = H_{in}V_{in} - h_{out}L_{out} = V_N(H_N - h_N) \quad (3.16)$$

3.4 Equations for the bottom section: (Stage n=2) (See Figure 3.4)

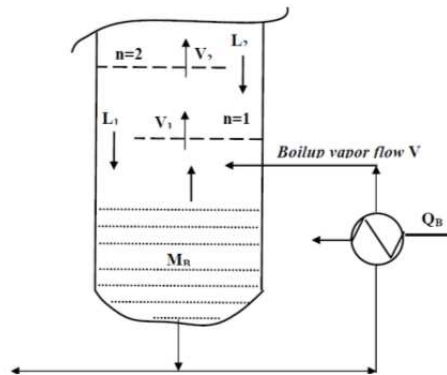


Fig. 3.4. Bottom Section and Re-boiler

Bottom Tray (stage n=2)

Total mass balance:

$$\frac{d(M_2)}{dt} = L_3 - L_2 + V_B - V_2 \quad (3.17)$$

Component balance:

$$\frac{d(M_2x_2)}{dt} = L_3x_3 - L_2x_2 + V_By_B - V_2y_2 \quad (3.18)$$

Energy balance:

$$\frac{d(M_Bh_B)}{dt} = h_3L_3 + H_BV_B - h_2L_2 - H_2V_2 \quad (3.19)$$

$$\Rightarrow V_2 = \frac{h_3L_3 + H_BV_B - (L_3 + V_B)h_2}{H_2 - h_2} \quad (3.20)$$

Re-boiler and Column Bottoms (stage n=1)

The base of the column has some particular characteristics as follows:

- There is re-boiler heat flux Q_B establishing the boil-up vapor flow V_B .

- The holdup is variable and changes in sensible heat cannot be neglected.
- The outflow of liquid from the bottoms B is determined externally to be controlled by a bottoms level controller.

Total mass balance:

$$\frac{d(M_B)}{dt} = L_2 - V_B - B \quad (3.21)$$

Component balance:

$$\frac{d(M_B x_B)}{dt} = L_2 x_2 - V_B y_B - B x_B \quad (3.22)$$

Energy balance:

$$\frac{d(M_B h_B)}{dt} = h_2 L_2 + Q_B - h_B B - H_B V_B \quad (3.23)$$

$$\Rightarrow V_B = \frac{h_2 L_2 + Q_B - h_B B - M_B \frac{dh_B}{dt} - h_B \frac{dM_B}{dt}}{H_B} \quad (3.24)$$

When all the modeling equations above are resolved, we find out how the flow rate and concentrations of the two product streams (distillate product and bottoms product) change with time, in the presence of changes in the various input variables.

3.5 Simplified model

To simplify the model, we make the following assumption (Papadouratis, A. *et al.* 1989):

- The relative volatility α is constant throughout the column. This means the vapor-liquid equilibrium relationship can be expressed by

$$y_n = \frac{\alpha x_n}{1 + (\alpha - 1)x_n} \quad (3.25)$$

where x_n : liquid composition on n^{th} stage; y_n : vapor composition on n^{th} stage; and α : relative volatility.

- The overhead vapor is totally condensed in a condenser.
- The liquid holdups on each tray, condenser, and the re-boiler are constant and perfectly mixed (i.e. immediate liquid response, $(dL_2 = dL_3 = \dots = dL_{N+2} = dL)$).
- The holdup of vapor is negligible throughout the system (i.e. immediate vapor response, $dV_1 = dV_2 = \dots = dV_{N+1} = dV$).
- The molar flow rates of the vapor and liquid through the stripping and rectifying sections are constant: $V_1 = V_2 = \dots = V_{N+1}$ and $L_2 = L_3 = \dots = L_{N+2}$.
- The column is numbered from bottom ($n=1$ for the re-boiler, $n=2$ for the first tray, $n=f$ for the feed tray, $n=N+1$ for the top tray and $n=N+2$ for the condenser).

Under these assumptions, the dynamic model can be expressed by (George, S., 1986):

Condenser ($n=N+2$):

$$M_D \dot{x}_n = (V + V_F)y_{n-1} - Lx_n - Dx_n \quad (3.26)$$

Tray n ($n=f+2, \dots, N+1$):

$$M \dot{x}_n = (V + V_F)(y_{n-1} - y_n) + L(x_{n+1} - x_n) \quad (3.27)$$

Tray above the feed flow ($n=f+1$):

$$M \dot{x}_n = V(y_{n-1} - y_n) + L(x_{n+1} - x_n) + V_F(y_F - y_n) \quad (3.28)$$

Tray below the feed flow ($n=f$):

$$M \dot{x}_n = V(y_{n-1} - y_n) + L(x_{n+1} - x_n) + L_F(x_F - x_n) \quad (3.29)$$

Tray n ($n=2, \dots, f-1$):

$$M \dot{x}_n = V(y_{n-1} - y_n) + (L + L_F)(x_{n+1} - x_n) \quad (3.30)$$

Re-boiler ($n=1$):

$$M_B \dot{x}_1 = (L + L_F)x_2 - Vy_1 - Bx_1 \quad (3.31)$$

Flow rate are assumed as constant molar flows as

$$L_F = q_F F \quad (3.32)$$

$$V_F = F - L_F \quad (3.33)$$

Assuming condenser holdup constant

$$D = V_N - L = V + V_F - L \quad (3.34)$$

Assuming boiler holdup constant

$$B = L_2 - V_1 = L + L_F - V \quad (3.35)$$

Composition x_F in the liquid and y_F in the vapor phase of the feed are obtained by solving the flash equations:

$$Fc_F = L_F x_F + V_F y_F \quad (3.36)$$

And

$$y_F = \frac{\alpha x_F}{1 + (\alpha - 1)x_F} \quad (3.37)$$

where, α is the relative volatility.

Although the model order is reduced, the representation of the distillation system is still *nonlinear* due to the vapor-liquid equilibrium relationship in equation (3.25).

4. Model simulation and analysis

4.1 Model dynamic equations

In the process data calculation, we have calculated for the distillation column with 14 trays with the following initial data - equations (2.1), (2.2), (2.3) and (2.4): The feed mass rate of the plant: $F_{mass} = 15.47619$ (tons/hour); The holdup in the column base: $M_B = 31.11$ (kmole);

The holdup on each tray: $M = 5.80$ (kmole); The holdup in the reflux drum: $M_D = 13.07$ (kmole); The gas percentage in the feed flow: $c_F = 38\%$; The internal vapor flow V_f selected by empirical: $V_f = 28\%$; The feed stream (m^3/h) with the density $d_F = 0.670$ (ton/m^3);

$F = \frac{F_{mass}}{d_F} = \frac{15.47619}{0.670} = 23.0988$ (m^3/h). The calculated stream data is displayed in the table 4.1.

Stream	Formular	%	Volume (m^3/h)	Density (ton/m^3)	Mass (ton/h)	Molar ($kg/kmol$)	Molar flow ($kmole/h$)
Vapor rate in feed V_F	c_{F+4}	42	9.7015	0.591	5.7336	58.2	98.5152
Liquid rate in feed L_F	$100-c_F$	58	13.3973	0.726	9.7264	93.3	104.2491
Internal vapor rate V	V_f	28	6.4677	0.598	3.8677	58.3	66.3407
Internal liquid rate L	V_f+4	32	7.3916	0.615	4.5458	60.1	75.6380
Distillate flow rate D	c_F	38	8.7775	0.576	5.0554	54.5	92.7597
Bottoms flow rate B	$100-c_F$	62	14.3213	0.727	10.405	93.8	110.9235

Table 4.1. Summary of Stream Data

Solving flash equation with the relative volatility ($\alpha = 5.68$), $\Rightarrow x_F = 0.26095$; $y_F = 0.66728$.

Reference to equations from (3.28) to (3.39) we can develop a set of nonlinear differential and algebraic equations for the simplified model can be developed as:

$$\begin{aligned} 13.07\dot{x}_{16} &= 164.8559y_{15} - 75.6380x_{16} - 92.7597x_{16} \\ &\Rightarrow \dot{x}_{16} = 12.6133y_{15} - 12.8863x_{16} \end{aligned} \quad (4.1)$$

$$\begin{aligned} 5.8\dot{x}_{15} &= 164.8559(y_{14} - y_{15}) + 75.6380(x_{16} - x_{15}) \\ &\Rightarrow \dot{x}_{15} = 28.4234y_{14} - 28.4234y_{15} + 13.0410x_{16} - 13.0410x_{15} \end{aligned} \quad (4.2)$$

$$\begin{aligned} 5.8\dot{x}_{14} &= 164.8559(y_{13} - y_{14}) + 75.6380(x_{15} - x_{14}) \\ &\Rightarrow \dot{x}_{14} = 28.4234y_{13} - 28.4234y_{14} + 13.0410x_{15} - 13.0410x_{14} \end{aligned} \quad (4.3)$$

$$\begin{aligned} 5.8\dot{x}_{13} &= 164.8559(y_{12} - y_{13}) + 75.6380(x_{14} - x_{13}) \\ \Rightarrow \dot{x}_{13} &= 28.4234y_{12} - 28.4234y_{13} + 13.0410x_{14} - 13.0410x_{13} \end{aligned} \quad (4.4)$$

$$\begin{aligned} 5.8\dot{x}_{12} &= 164.8559(y_{11} - y_{12}) + 75.6380(x_{13} - x_{12}) \\ \Rightarrow \dot{x}_{12} &= 28.4234y_{11} - 28.4234y_{12} + 13.0410x_{13} - 13.0410x_{12} \end{aligned} \quad (4.5)$$

$$\begin{aligned} 5.8\dot{x}_{11} &= 164.8559(y_{10} - y_{11}) + 75.6380(x_{12} - x_{11}) \\ \Rightarrow \dot{x}_{11} &= 28.4234y_{10} - 28.4234y_{11} + 13.0410x_{12} - 13.0410x_{11} \end{aligned} \quad (4.6)$$

$$\begin{aligned} 5.8\dot{x}_{10} &= 164.8559(y_9 - y_{10}) + 75.6380(x_{11} - x_{10}) \\ \Rightarrow \dot{x}_{10} &= 28.4234y_9 - 28.4234y_{10} + 13.0410x_{11} - 13.0410x_{10} \end{aligned} \quad (4.7)$$

$$\begin{aligned} 5.8\dot{x}_9 &= 66.3407(y_8 - y_9) + 75.6380(x_{10} - x_9) + 98.5152(0.66728 - y_9) \\ \Rightarrow \dot{x}_9 &= 11.4381y_8 - 28.4234y_9 - 13.0410x_9 + 13.0410x_{10} + 11.3340 \end{aligned} \quad (4.8)$$

$$\begin{aligned} 5.8\dot{x}_8 &= 66.3407(y_7 - y_8) + 75.6380(x_9 - x_8) + 104.2491(0.26.95 - x_8) \\ \Rightarrow \dot{x}_8 &= 11.4381y_7 - 11.4381y_8 - 31.0150x_8 + 13.0410x_9 + 4.8440 \end{aligned} \quad (4.9)$$

$$\begin{aligned} 5.8\dot{x}_7 &= 66.3407(y_6 - y_7) + 179.8871(x_8 - x_7) \\ \Rightarrow \dot{x}_7 &= 11.4381y_6 - 11.4381y_7 + 31.0150x_8 - 31.0150x_7 \end{aligned} \quad (4.10)$$

$$\begin{aligned} 5.8\dot{x}_6 &= 66.3407(y_5 - y_6) + 179.8871(x_7 - x_6) \\ \Rightarrow \dot{x}_6 &= 11.4381y_5 - 11.4381y_6 + 31.0150x_7 - 31.0150x_6 \end{aligned} \quad (4.11)$$

$$\begin{aligned} 5.8\dot{x}_5 &= 66.3407(y_4 - y_5) + 179.8871(x_6 - x_5) \\ \Rightarrow \dot{x}_5 &= 11.4380y_4 - 11.4381y_5 + 31.0150x_6 - 31.0150x_5 \end{aligned} \quad (4.12)$$

$$\begin{aligned} 5.8\dot{x}_4 &= 66.3407(y_3 - y_4) + 179.8871(x_5 - x_4) \\ \Rightarrow \dot{x}_4 &= 11.4381y_3 - 11.4381y_4 + 31.0150x_5 - 31.0150x_4 \end{aligned} \quad (4.13)$$

$$\begin{aligned} 5.8\dot{x}_3 &= 66.3407(y_2 - y_3) + 179.8871(x_4 - x_3) \\ \Rightarrow \dot{x}_3 &= 11.4381y_2 - 11.4381y_3 + 31.0150x_4 - 31.0150x_3 \end{aligned} \quad (4.14)$$

$$\begin{aligned} 5.8\dot{x}_2 &= 66.3407(y_1 - y_2) + 179.8871(x_3 - x_2) \\ \Rightarrow \dot{x}_2 &= 11.4381y_1 - 11.4381y_2 + 31.0150x_3 - 31.0150x_2 \end{aligned} \quad (4.15)$$

$$\begin{aligned} 31.11\dot{x}_1 &= 179.8871x_2 - 110.9235x_1 - 66.3407y_1 \\ \Rightarrow \dot{x}_1 &= -3.5655x_1 + 5.7823x_2 - 2.1325y_1 \end{aligned} \quad (4.16)$$

And vapor-liquid equilibrium on each tray ($n=1-16$):

$$y_n = \frac{5.68x_n}{1 + 4.68x_n} \quad (4.17)$$

4.2 Model simulation with Matlab Simulink

4.2.1 Simulation without disturbances

The steady-state solution is determined with dynamic simulation. Figure 4.1 displays the concentration of the light component x_n at each tray and Table 4.2 shows the steady state values of concentration of x_n on each tray.

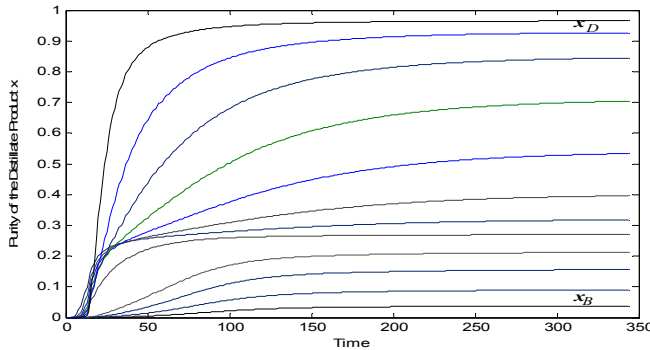


Fig. 4.1. Steady state values of concentration x_n on each tray

Tray	1	2	3	4	5	6	7	8
x_n	0.0375	0.0900	0.1559	0.2120	0.2461	0.2628	0.2701	0.2731
y_n	0.1812	0.3597	0.5120	0.6044	0.6496	0.6694	0.6776	0.6809
Tray	9	10	11	12	13	14	15	16
x_n	0.2811	0.3177	0.3963	0.5336	0.7041	0.8449	0.9269	0.9654
y_n	0.6895	0.7256	0.7885	0.8666	0.9311	0.9687	0.9863	0.9937

Table 4.2. Steady state values of concentration x_n on each tray

If there are no disturbance in operating condition, the system model is to achieve the steady state of product quality that the purity of the distillate product $x_D = 0.9654$ and the impurity of the bottoms product $x_B = 0.0375$.

4.2.2 Simulation with 10% decreasing and increasing feed flow rate

When decreasing the feed flow rate by 10%, the quality of the distillate product will get worse while the quality of the bottoms product will get better: the purity of the distillate product reduces from 96.54% to 90.23% while the impurity of the bottoms product reduces from 3.75% to 0.66%.

In contrast, when increasing the feed flow rate by 10%, the quality of the distillate product will be better while the quality of the bottoms product will be worse: the purity of the distillate product increases from 96.54% to 97.30% while the impurity of the bottoms product increases from 3.75% to 11.66%. (See Table 4.3 and Figure 4.2).

	Purity of the Distillate Product (%)	Impurity of the Bottoms Product (%)
Normal Feed Rate (100%)	96.54	3.75
Reduced Feed Rate (90%)	90.23	0.66
Increased Feed Rate (110%)	97.30	11.66

Table 4.3. Product quality depending on the change of feed rate

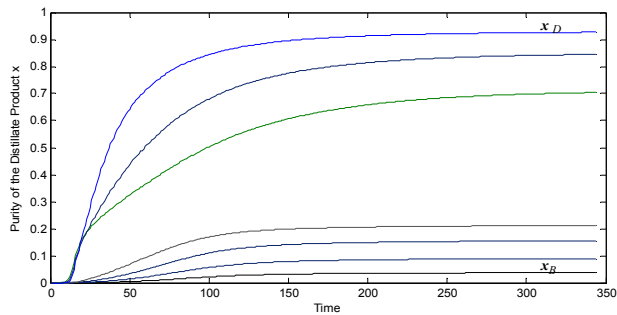


Fig. 4.2. Product qualities depending on change of feed rate

4.2.3 Simulation with a wave change in the feed flow rate by $\pm 5\%$

When the input flow rate fluctuates in a *sine wave* by $\pm 5\%$ (see Figure 4.3), the purity of the distillate product and the impurity of the bottoms product will also fluctuate in a sine wave (see Figure 4.4 and Table 4.4).

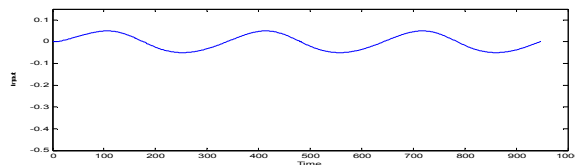


Fig. 4.3. Feed flow rate in a sine wave around $\pm 5\%$

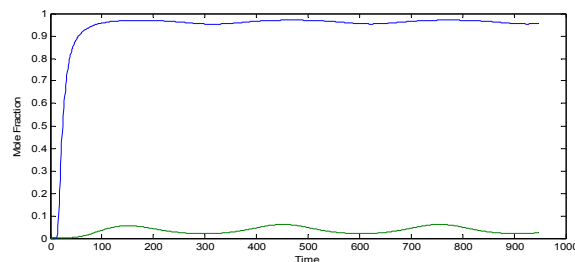


Fig. 4.4. Product quality for a sine wave feed rate

	Feed Flow Rate (%)	Distillate Purity (%)	Bottoms Impurity (%)
Max Value	105	96.92	5.53
Min Value	95	95.26	2.06

Table 4.4. Product quality depending on the input sine wave fluctuation

The product quality of this feed rate is not satisfied with $x_B \geq 96\%$ and $x_D \leq 4\%$.

5. Linearized control model

5.1 Linear approximation of nonlinear system

5.1.1 Vapor-Liquid equilibrium relationship in each tray

$$y_n = \frac{\alpha x_n}{1 + (\alpha - 1)x_n} = \frac{5.68x_n}{1 + 4.68x_n} \quad (5.1)$$

In order to obtain a linear mathematical model for a nonlinear system, it is assumed that the variables deviate only slightly from some operating condition (Ogata, K., 2001). If the normal operating condition corresponds to \bar{x}_n and \bar{y}_n , then equation (5.1) can be expanded into a Taylor's series as:

$$y_n = f(\bar{x}_n) + \frac{df}{dx_n}(x_n - \bar{x}_n) + \frac{1}{2!} \frac{d^2f}{dx_n^2}(x_n - \bar{x}_n)^2 + \dots \quad (5.2)$$

where the derivatives df/dx_n , d^2f/dx_n^2 , ... are evaluated at $x_n = \bar{x}_n$. If the variation $x_n - \bar{x}_n$ is small, the higher-order terms in $x_n - \bar{x}_n$ may be neglected. Then equation (5.2) can be written as:

$$y_n = \bar{y}_n + K_n(x_n - \bar{x}_n) \text{ with } \bar{y}_n = f(\bar{x}_n) \text{ and } K = \left. \frac{df}{dx_n} \right|_{x_n = \bar{x}_n} \quad (5.3)$$

From (5.3), equation (5.1) can be written:

$$y_n = \bar{y}_n + K_n(x_n - \bar{x}_n) \text{ with } \bar{y}_n = \frac{5.68\bar{x}_n}{1 + 4.68\bar{x}_n} \text{ and } K_n = \frac{5.68}{(1 + 4.68\bar{x}_n)^2} \quad (5.4)$$

Tray	1	2	3	4	5	6	7	8
x_n	0.0375	0.0900	0.1559	0.2120	0.2461	0.2628	0.2701	0.2731
y_n	0.1812	0.3597	0.5120	0.6044	0.6496	0.6694	0.6776	0.6809
K_n	4.1106	2.8121	1.8987	1.4312	1.2268	1.1423	1.1081	1.0945
Tray	9	10	11	12	13	14	15	16
x_n	0.2811	0.3177	0.3963	0.5336	0.7041	0.8449	0.9269	0.9654
y_n	0.6895	0.7256	0.7885	0.8666	0.9311	0.9687	0.9863	0.9937
K_n	1.0594	0.9184	0.6970	0.4644	0.3079	0.2314	0.1993	0.1865

Table 5.1. The Concentration x_n , y_n and the linearization coefficient K_n

5.1.2 Material balance relationship in each tray

Linearization for general trays ($n = 2 \div 15$) - ACCUMULATION = INLET - OUTLET:

$$\begin{aligned}
 M_n \dot{x}_n &= (V_{n-1}y_{n-1} + L_{n+1}x_{n+1}) - (V_n y_n + L_n x_n) \\
 \Rightarrow \dot{x}_n &= \frac{V_{n-1}}{M_n} y_{n-1} - \frac{V_n}{M_n} y_n + \frac{L_{n+1}}{M_n} x_{n+1} - \frac{L_n}{M_n} x_n
 \end{aligned}
 \tag{5.5}$$

where,

$$\begin{aligned}
 L_1 = L_2 = \dots = L_{F-1} = L + L_F; L_{F+2} = L_{F+3} = \dots = L; V_1 = V_2 = \dots = V_{F-1} = V; \\
 V_{F+2} = V_{F+3} = \dots = V_{N+1} = V + V_F; M_n = M = 5.8; V_{Steady\ State} = \bar{V} = 66.3407; \\
 L_{Steady\ State} = \bar{L} = 75.6380; L_F = 104.2491; V_F = 98.5152.
 \end{aligned}$$

Substituting equation (5.4) into equation (5.5), the following expression is obtained:

$$\dot{x}_n = \frac{(\bar{y}_{n-1} - K_{n-1}\bar{x}_{n-1})V_{n-1}}{M_n} + \frac{(K_{n-1})V_{n-1}x_{n-1}}{M_n} - \frac{(\bar{y}_n - K_n\bar{x}_n)V_n}{M_n} - \frac{(K_n)V_n x_n}{M_n} + \frac{L_{n+1}x_{n+1}}{M_n} - \frac{L_n x_n}{M_n}$$

In order to obtain a linear approximation to this nonlinear system, this equation may be expanded into a Taylor series about the normal operating point from equation (5.3), and the linear approximation equations for general trays are obtained:

$$\begin{aligned}
 \dot{x}_n - \bar{x}_n &= \frac{(K_{n-1}\bar{V}_n)}{M} x_{n-1} - \frac{(K_n\bar{V}_n + \bar{L}_n)}{M} x_n + \frac{(\bar{L}_n)}{M} x_{n+1} + \frac{(\bar{x}_{n+1} - \bar{x}_n)L}{M} - \frac{(\bar{y}_n - \bar{y}_{n-1})V}{M} \\
 &\quad - \frac{\bar{L}_n(\bar{x}_{n+1} - \bar{x}_n)}{M} + \frac{\bar{V}_n(K_n\bar{x}_n - K_{n-1}\bar{x}_{n-1})}{M}
 \end{aligned}
 \tag{5.6}$$

Linearization for special trays:

Tray above the feed flow ($n=f+1$): $\dot{x}_n = \frac{(y_{n-1} - y_n)V}{M} + \frac{(x_{n+1} - x_n)L}{M} + \frac{(y_F - y_n)V_F}{M}$ and the linear approximation equations for the tray above the feed flow:

$$\begin{aligned}
 \dot{x}_n - \bar{x}_n &= \frac{(K_{n-1}\bar{V})}{M} x_{n-1} - \frac{(K_n\bar{V} + L + K_n V_F)}{M} x_n + \frac{\bar{L}}{M} x_{n+1} + \frac{(\bar{x}_{n+1} - \bar{x}_n)L}{M} + \frac{(\bar{y}_n - \bar{y}_{n-1})V}{M} \\
 &\quad - \frac{\bar{L}(\bar{x}_{n+1} - \bar{x}_n)}{M} + \frac{\bar{V}(K_n\bar{x}_n - K_{n-1}\bar{x}_{n-1}) + V_F(y_F - \bar{y}_n + K_n\bar{x}_n)}{M}
 \end{aligned}
 \tag{5.7}$$

Tray below the feed flow ($n=f$): $\dot{x}_n - \bar{x}_n = \frac{(y_{n-1} - y_n)V}{M} + \frac{(x_{n+1} - x_n)L}{M} + \frac{(x_F - x_n)L_F}{M}$ and the linear approximation equations for the tray above the feed flow:

$$\begin{aligned}
 \dot{x}_n - \bar{x}_n &= \frac{(K_{n-1}\bar{V})}{M} x_{n-1} + \frac{(K_n\bar{V} + \bar{L} + L_F)}{M} x_n + \frac{\bar{L}}{M} x_{n+1} + \frac{(\bar{x}_{n+1} - \bar{x}_n)L}{M} - \frac{(\bar{y}_n - \bar{y}_{n-1})V}{M} \\
 &\quad - \frac{\bar{L}(\bar{x}_{n+1} - \bar{x}_n) - L_F x_F}{M} + \frac{\bar{V}(K_n\bar{x}_n - K_{n-1}\bar{x}_{n-1})}{M}
 \end{aligned}
 \tag{5.8}$$

Reboiler ($n=1$): $\dot{x}_1 = \frac{L_2 x_2}{M_B} - \frac{V y_1}{M_B} - \frac{B x_1}{M_B}$, where, $M_B = 31.11$ a, $B = 110.9235$, and the linear approximation equations for the reboiler:

$$\dot{x}_1 - \bar{x}_1 = -\frac{(K_1 \bar{V} + B)}{M_B} x_1 + \frac{(\bar{L} + \bar{L}_F)}{M_B} x_2 + \frac{(\bar{x}_2)_L}{M_B} L - \frac{(\bar{y}_1)_V}{M_B} V - \frac{((\bar{L} + L_F) \bar{x}_2)}{M_B} + \frac{(\bar{V} K_1 \bar{x}_1)}{M_B} \quad (5.9)$$

Condenser ($n=N$): $\dot{x}_{16} = \frac{V_{15} y_{15}}{M_D} - \frac{L x_{16}}{M_D} - \frac{D x_{16}}{M_D}$, where, $M_D = 13.07$, $D = 92.7597$, and the linear approximation equations for the condenser:

$$\dot{x}_{16} - \bar{x}_{16} = \frac{(K_{15}(\bar{V} + V_F))}{M_D} x_{15} - \frac{(\bar{L} + D)}{M_D} x_{16} - \frac{(\bar{x}_{16})_L}{M_D} L + \frac{(\bar{y}_{15})_V}{M_D} V + \frac{(\bar{L} \bar{x}_{16})}{M_D} - \frac{((\bar{V} + V_F) K_{15} \bar{x}_{15})}{M_D} \quad (5.10)$$

As a result, the model is represented in state space in terms of deviation variables:

$$\begin{aligned} \dot{z}(t) &= Az(t) + Bu(t) \\ y(t) &= Cz(t) \end{aligned}, \text{ where}$$

$$z(t) = \begin{bmatrix} x_1(t) - \bar{x}_1 \text{ Steady State} \\ x_2(t) - \bar{x}_2 \text{ Steady State} \\ \vdots \\ x_{16}(t) - \bar{x}_{16} \text{ Steady State} \end{bmatrix}, \quad (5.11)$$

$$u(t) = \begin{bmatrix} L(t) - \bar{L}_{\text{Steady State}} = dL \\ V(t) - \bar{V}_{\text{Steady State}} = dV \end{bmatrix}, \quad y(t) = \begin{bmatrix} x_1(t) - \bar{x}_1 \text{ Steady State} = dx_B \\ x_{16}(t) - \bar{x}_{16} \text{ Steady State} = dx_D \end{bmatrix}$$

The matrix A elements:

$$\text{For } n=1, a_{1,1} = -\frac{(K_1 \bar{V} + B)}{M_B}, a_{1,2} = \frac{(\bar{L} + \bar{L}_F)}{M_B}$$

$$\text{For } n=2 \div 7, a_{n,n-1} = \frac{(K_{n-1} \bar{V})}{M}, a_{n,n} = -\frac{(K_n \bar{V} + \bar{L} + L_F)}{M}, a_{n,n+1} = \frac{(\bar{L} + L_F)}{M}$$

$$\text{For } n=8, a_{8,7} = \frac{(K_7 \bar{V})}{M}, a_{8,8} = -\frac{(K_8 \bar{V} + \bar{L} + L_F)}{M}, a_{8,9} = \frac{(\bar{L})}{M}$$

$$\text{For } n=9, a_{9,8} = \frac{(K_8 \bar{V})}{M}, a_{9,9} = -\frac{(K_9 \bar{V} + \bar{L})}{M}, a_{9,10} = \frac{(\bar{L})}{M}$$

$$\text{For } n=10 \div 15, a_{n,n-1} = \frac{(K_{n-1}(\bar{V} + V_F))}{M}, a_{n,n} = -\frac{(K_n(\bar{V} + V_F) + \bar{L})}{M}, a_{n,n+1} = \frac{(\bar{L})}{M}$$

$$\text{For } n=16, a_{16,15} = \frac{(K_{15}(\bar{V} + V_F))}{M_D}, a_{16,16} = -\frac{(\bar{L} + D)}{M_D}, \text{ then:}$$

$$A = \begin{pmatrix} -12.3312 & 5.7823 & 0 & 0 & 0 & 0 & 0 & 0 & 0 & 0 & 0 & 0 & 0 & 0 & 0 & 0 & 0 & 0 \\ 47.0173 & -63.1800 & 31.0150 & 0 & 0 & 0 & 0 & 0 & 0 & 0 & 0 & 0 & 0 & 0 & 0 & 0 & 0 & 0 \\ 0 & 32.1649 & -52.7324 & 31.0150 & 0 & 0 & 0 & 0 & 0 & 0 & 0 & 0 & 0 & 0 & 0 & 0 & 0 & 0 \\ 0 & 0 & 21.7174 & -47.3852 & 31.0150 & 0 & 0 & 0 & 0 & 0 & 0 & 0 & 0 & 0 & 0 & 0 & 0 & 0 \\ 0 & 0 & 0 & 16.3701 & -45.0472 & 31.0150 & 0 & 0 & 0 & 0 & 0 & 0 & 0 & 0 & 0 & 0 & 0 & 0 \\ 0 & 0 & 0 & 0 & 14.0322 & -44.0807 & 31.0150 & 0 & 0 & 0 & 0 & 0 & 0 & 0 & 0 & 0 & 0 & 0 \\ 0 & 0 & 0 & 0 & 0 & 13.0657 & -43.6895 & 31.0150 & 0 & 0 & 0 & 0 & 0 & 0 & 0 & 0 & 0 & 0 \\ 0 & 0 & 0 & 0 & 0 & 0 & 12.6745 & -43.5340 & 13.0410 & 0 & 0 & 0 & 0 & 0 & 0 & 0 & 0 & 0 \\ 0 & 0 & 0 & 0 & 0 & 0 & 0 & 12.5189 & -43.1528 & 13.0410 & 0 & 0 & 0 & 0 & 0 & 0 & 0 & 0 \\ 0 & 0 & 0 & 0 & 0 & 0 & 0 & 0 & 30.1118 & -39.1451 & 13.0410 & 0 & 0 & 0 & 0 & 0 & 0 & 0 \\ 0 & 0 & 0 & 0 & 0 & 0 & 0 & 0 & 0 & 26.1041 & -32.8522 & 13.0410 & 0 & 0 & 0 & 0 & 0 & 0 \\ 0 & 0 & 0 & 0 & 0 & 0 & 0 & 0 & 0 & 0 & 19.8111 & -26.2409 & 13.0410 & 0 & 0 & 0 & 0 & 0 \\ 0 & 0 & 0 & 0 & 0 & 0 & 0 & 0 & 0 & 0 & 0 & 13.1998 & -21.7926 & 13.0410 & 0 & 0 & 0 & 0 \\ 0 & 0 & 0 & 0 & 0 & 0 & 0 & 0 & 0 & 0 & 0 & 0 & 8.7516 & -19.6182 & 13.0410 & 0 & 0 & 0 \\ 0 & 0 & 0 & 0 & 0 & 0 & 0 & 0 & 0 & 0 & 0 & 0 & 0 & 6.5772 & -18.7058 & 13.0410 & 0 & 0 \\ 0 & 0 & 0 & 0 & 0 & 0 & 0 & 0 & 0 & 0 & 0 & 0 & 0 & 0 & 0 & 2.5138 & -12.8843 & 0 \end{pmatrix}$$

The matrix B elements:

For n=1, $b_{1,1} = \frac{(\bar{x}_2)}{M_B}L$, $b_{1,2} = -\frac{(\bar{y}_1)}{M_B}V$

For n=2÷15, $b_{n,1} = \frac{(\bar{x}_{n+1} - \bar{x}_n)}{M}L$, $b_{n,2} = -\frac{(\bar{y}_n - \bar{y}_{n-1})}{M}V$

For n=16, $b_{16,1} = -\frac{(\bar{x}_{16})}{M_D}L$, $b_{16,2} = \frac{(\bar{y}_{15})}{M_D}V$, then:

$$B = \begin{pmatrix} 0.0029 & -0.0058 \\ 0.0114 & -0.0308 \\ 0.0097 & -0.0263 \\ 0.0059 & -0.0159 \\ 0.0029 & -0.0078 \\ 0.0013 & -0.0034 \\ 0.0005 & -0.0014 \\ 0.0014 & -0.0006 \\ 0.0063 & -0.0015 \\ 0.0136 & -0.0062 \\ 0.0237 & -0.0108 \\ 0.0294 & -0.0135 \\ 0.0243 & -0.0111 \\ 0.0141 & -0.0065 \\ 0.0066 & -0.0030 \\ -0.0739 & 0.0755 \end{pmatrix}$$

And the output matrix C is:

$$C = \begin{pmatrix} 1 & 0 & 0 & 0 & 0 & 0 & 0 & 0 & 0 & 0 & 0 & 0 & 0 & 0 & 0 & 0 & 0 & 0 \\ 0 & 0 & 0 & 0 & 0 & 0 & 0 & 0 & 0 & 0 & 0 & 0 & 0 & 0 & 0 & 0 & 0 & 1 \end{pmatrix}$$

5.2 Reduced-order linear model

The full-order linear model in equation 5-11, which represents a 2 input – 2 output plant can be expressed in the S domain as:

$$\begin{vmatrix} dx_D \\ dx_B \end{vmatrix} = \frac{1}{1 + \tau_c s} G(0) \begin{vmatrix} dL \\ dV \end{vmatrix} \quad (5.12)$$

where τ_c is the time constant and $G(0)$ is the steady state gain

The steady state gain can be directly calculated: $G(0) = -CA^{-1}B$ or

$$G(0) = \begin{vmatrix} 0.0042 & -0.0060 \\ -0.0050 & 0.0072 \end{vmatrix} \quad (5.13)$$

The time constant τ_c can be calculated based on some specified assumptions (Skogestad, S., & Morari, M., 1987). The linearized value of τ_c is given by:

$$\tau_c = \frac{M_I}{I_s \ln S} + \frac{M_D(1-x_D)x_D}{I_s} + \frac{M_B(1-x_B)x_B}{I_s} \quad (5.14)$$

where M_I is the total holdup of liquid inside the column:

$$M_I = \sum_{i=1}^N M_i = 5.8 * 14 = 81.2 \text{ (kmole);}$$

I_s is the "impurity sum": $I_s = D(1-x_D)x_D + B(1-x_B)x_B = 7.1021$, and S is the separation factor: $S = \frac{x_D(1-x_B)}{(1-x_D)x_B} = 716.1445$.

So that, the time constant τ_c in equation (5.14) can be determined: $\tau_c = 1.9588$ (h).

As the result, the reduced-order model of the plant is a first order system in equation (5.12):

$$\begin{vmatrix} dx_D \\ dx_B \end{vmatrix} = \frac{1}{1 + 1.9588s} \begin{vmatrix} 0.0042 & -0.0060 \\ -0.0050 & 0.0072 \end{vmatrix} \begin{vmatrix} dL \\ dV \end{vmatrix} \quad (5.15)$$

or the equivalent reduced-order model in state space:

$$\begin{aligned} \dot{z}_r(t) &= \begin{vmatrix} -0.5105 & 0 \\ 0 & -0.5105 \end{vmatrix} z_r(t) + \begin{vmatrix} 1 & 0 \\ 0 & 1 \end{vmatrix} u(t) \\ y_r(t) &= \begin{vmatrix} 0.0021 & -0.0031 \\ -0.0026 & 0.0037 \end{vmatrix} z_r(t) \end{aligned} \quad (5.16)$$

6. Control simulation with MRAC

The reduced-order linear model is then used as the reference model for a model-reference adaptive control (MRAC) system to verify the applicable ability of a conventional adaptive

controller for a distillation column dealing with the disturbance and the model-plant mismatch as the influence of the plant feed disturbances.

Adaptive control system is the ability of a controller which can adjust its parameters in such a way as to compensate for the variations in the characteristics of the process. Adaptive control is widely applied in petroleum industries because of the two main reasons: Firstly, most processes are nonlinear and the linearized models are used to design the controllers, so that the controller must change and adapt to the model-plant mismatch; Secondly, most of the processes are non-stationary or their characteristics are changed with time, this leads again to adapt the changing control parameters.

The general form of a MRAC is based on an inner-loop Linear Model Reference Controller (LMRC) and an outer adaptive loop shown in Fig. 6.1. In order to eliminate errors between the model, the plant and the controller is asymptotically stable, MRAC will calculate online the adjustment parameters in gains L and M by $\theta_L(t)$ and $\theta_M(t)$ as detected state error $e(t)$ when changing A, B in the process plant.

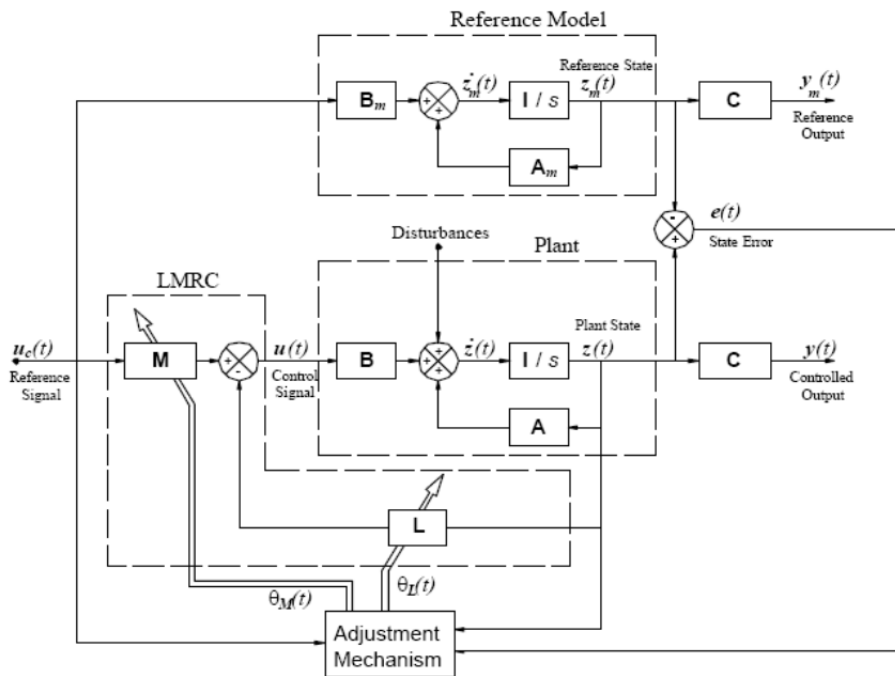


Fig. 6.1. MRAC block diagram

Simulation program is constructed using Maltab Simulink with the following data:

Process Plant:

$$\dot{z} = Az + Bu + noise$$

$$y = Cz$$

where $A = \begin{bmatrix} \alpha_1 & 0 \\ 0 & \alpha_2 \end{bmatrix}$, $B = \begin{bmatrix} \beta_1 & 0 \\ 0 & \beta_2 \end{bmatrix}$, $C = \begin{bmatrix} 0.004 & -0.007 \\ -0.0011 & 0.0017 \end{bmatrix}$ and $\alpha_1, \alpha_2, \beta_1, \beta_2$ are changing and dependent on the process dynamics.

Reference Model:

$$\begin{aligned} \dot{z}_m &= A_m z_m + B_m u_c \\ y_m &= C_m z_m \end{aligned}$$

where $A_m = \begin{bmatrix} -0.2616 & 0 \\ 0 & -0.2616 \end{bmatrix}$, $B_m = \begin{bmatrix} 1 & 0 \\ 0 & 1 \end{bmatrix}$, $C_m = \begin{bmatrix} 0.004 & -0.007 \\ -0.0011 & 0.0017 \end{bmatrix}$

State Feedback:

$$u = Mu_c - Lz \text{ where } L = \begin{bmatrix} \theta_1 & 0 \\ 0 & \theta_2 \end{bmatrix} \text{ and } M = \begin{bmatrix} \theta_3 & 0 \\ 0 & \theta_4 \end{bmatrix}.$$

Closed Loop:

$$\dot{z} = (A - BL)z + BMu_c = A_c(\theta)z + B_c(\theta)u_c$$

Error Equation:

$e = z - z_m = \begin{bmatrix} e_1 \\ e_2 \end{bmatrix}$ is a vector of state errors,

$$\dot{e} = \dot{z} - \dot{z}_m = Az + Bu - A_m z_m - B_m u_c = A_m e + (A_c(\theta) - A_m)z + (B_c(\theta) - B_m)u_c = A_m e + \Psi(\theta - \theta^0)$$

where $\Psi = \begin{bmatrix} -\beta_1 z_1 & 0 & \beta_1 u_{c1} & 0 \\ 0 & -\beta_2 z_2 & 0 & \beta_2 u_{c2} \end{bmatrix}$

Lyapunov Function:

$V(e, \theta) = \frac{1}{2} (\gamma e^T P e + (\theta - \theta^0)^T (\theta - \theta^0))$ where γ is an adaptive gain and P is a Lyapunov matrix.

Derivative Calculation of Lyapunov Matrix:

$$\frac{dV}{dt} = -\frac{\gamma}{2} e^T Q e + (\theta - \theta^0)^T \left(\frac{d\theta}{dt} + \gamma \Psi^T P e \right) \text{ where } Q = -A_m^T P - P A_m.$$

For the stability of the system, $\frac{dV}{dt} < 0$, we can assign the second item

$$(\theta - \theta^0)^T \left(\frac{d\theta}{dt} + \gamma \Psi^T P e \right) = 0 \text{ or } \frac{d\theta}{dt} = -\gamma \Psi^T P e. \text{ Then we always have: } \frac{dV}{dt} = -\frac{\gamma}{2} e^T Q e. \text{ If we}$$

select a positive matrix $P > 0$, for instance, $P = \begin{bmatrix} 1 & 0 \\ 0 & 2 \end{bmatrix}$, then we have

$Q = -A_m^T P - P A_m = \begin{bmatrix} 0.5232 & 0 \\ 0 & 1.0465 \end{bmatrix}$. Since matrix Q is obviously positive definite, then we always have $\frac{dV}{dt} = -\frac{\gamma}{2} e^T Q e < 0$ and the system is stable with any plant-model mismatches.

Parameters Adjustment:

$$\frac{d\theta}{dt} = -\gamma \begin{bmatrix} -\beta_1 z_1 & 0 \\ 0 & -\beta_2 z_2 \\ \beta_{c1} u_1 & 0 \\ 0 & \beta_2 u_{2c} \end{bmatrix} [P] \begin{bmatrix} e_1 \\ e_2 \end{bmatrix} = \begin{bmatrix} d\theta_1 / dt \\ d\theta_2 / dt \\ d\theta_3 / dt \\ d\theta_4 / dt \end{bmatrix} = \begin{bmatrix} \gamma \beta_1 z_1 e_1 \\ 2\gamma \beta_2 z_2 e_2 \\ -\gamma \beta_1 u_{c1} e_1 \\ -2\gamma \beta_2 u_{c2} e_2 \end{bmatrix}$$

Simulation results and analysis:

It is assumed that the reduced-order linear model in equation (11) can also maintain the similar steady state outputs as the basic nonlinear model. Now this model is used as an MRAC to take the process plant from these steady state outputs ($x_D = 0.9654$ and $x_B = 0.0375$) to the desired targets ($0.98 \leq x_D \leq 1$ and $0 \leq x_B \leq 0.02$) amid the disturbances and the plant-model mismatches as the influence of the feed stock disturbances.

The design of a new adaptive controller is shown in Figure 6.2 where we install an MRAC and a closed-loop PID (Proportional, Integral, Derivative) controller to eliminate the errors between the reference set-points and the outputs.

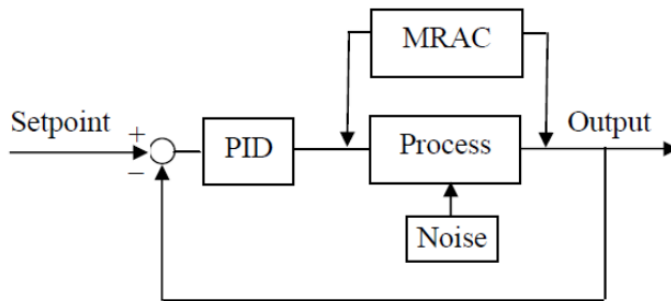


Fig. 6.2. Adaptive controller with MRAC and PID

This controller system was run with different plant-model mismatches, for instance, a plant with $A = \begin{bmatrix} -0.50 & 0 \\ 0 & -0.75 \end{bmatrix}$, $B = \begin{bmatrix} 1.5 & 0 \\ 0 & 2.5 \end{bmatrix}$ and an adaptive gain $\gamma = 25$. The operating setpoints for the real outputs are $x_{DR} = 0.99$ and $x_{BR} = 0.01$. Then, the reference set-points for the PID controller are $r_D = 0.0261$ and $r_B = -0.0275$ since the real steady state outputs are $x_D = 0.9654$ and $x_B = 0.0375$. Simulation in Figure 6.2 shows that the controlled outputs x_D and x_B are always stable and tracking to the model outputs and the reference set-points (the dotted lines, r_D and r_B) amid the disturbances and the plant-model mismatches (Figure 6.3).

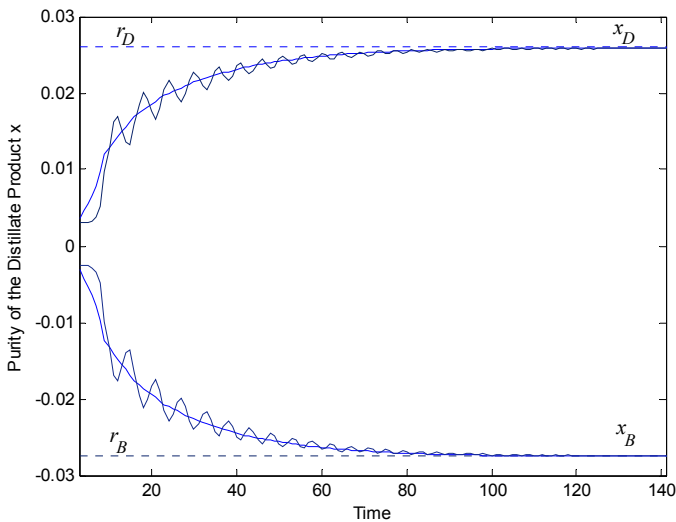


Fig. 6.3. Correlation of Plant Outputs, Model Outputs and Reference Setpoints

7. Conclusion

A procedure has been introduced to build up a mathematical model and simulation for a condensate distillation column based on the energy balance ($L-V$) structure. The mathematical modeling simulation is accomplished over three phases: the basic nonlinear model, the full order linearized model and the reduced order linear model. Results from the simulations and analysis are helpful for initial steps of a petroleum project feasibility study and design.

The reduced order linear model is used as the reference model for an MRAC controller. The controller of MRAC and PID theoretically allows the plant outputs tracking the reference set-points to achieve the desired product quality amid the disturbances and the model-plant mismatches as the influence of the feed stock disturbances.

In this chapter, the calculation of the mathematical model building and the reduced-order linear adaptive controller is only based on the physical laws from the process. The real system identifications including the experimental production factors, specific designed structures, parameters estimation and the system validation are not discussed here.

8. Acknowledgment

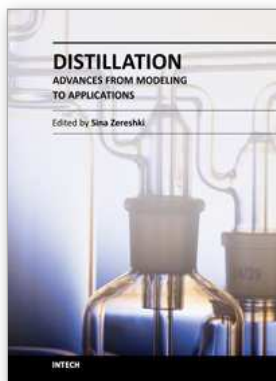
The authors would like to thank InTech for providing the opportunity to print this book chapter. Special thanks are also due to the anonymous reviewers and editor, who assisted the author in improving this book chapter significantly. Lastly, the authors would like to thank the Papua New Guinea University of Technology (UNITECH) for their support in the preparation of this book chapter.

9. References

- Franks, R. (1972), *Modeling and Simulation in Chemical Engineering*, Wiley-Interscience, New York, ISBN: 978-0471275350.
- George, S. (1986). *Chemical Process Control: An Introduction to Theory and Practice*, Prentice-Hall, ISBN: 9780131286290, New Jersey.
- Kehlen, H. & Ratzsch, M. (1987). Complex Multicomponent Distillation Calculations by Continuous Thermodynamics. *Chem. Eng. Sci.*, Vol. 42(2), pp. 221-232 ISSN: 0009-2509.
- Luyben, W. (1990). *Process Modeling, Simulation, and Control for Chemical Engineers*, McGraw-Hill, ISBN: 978-0070391598, New York.
- Marie, E.; Strand, S. & Skogestad S. (2008). Coordinator MPC for Maximizing Plant Throughput. *Computer & Chemical Engineering*, Vol. 32(2), pp. 195-204, ISSN: 0098-1354.
- Nelson, W. (1985), *Petroleum Refinery Engineering*, McGraw-Hill, ISBN: 978-0-8247-0599-2, Singapore.
- Ogata, K. (2001). *Modern Control Engineering*, Prentice Hall, ISBN: 978-0130609076, New York.
- Papadouratis, A.; Doherty, M. & Douglas, J. (1989). Approximate Dynamic Models for Chemical Process Systems. *Ind. & Eng. Ch. Re.*, Vol. 28(5), pp. 546-522, ISSN: 0888-5885.
- Perry, R. & Green, D. (1984). *Perry's Chemical Engineers Handbook*, McGraw-Hill, ISBN: 0-471-58626-9, New York.
- PetroVietnam Gas Company. (1999), *Condensate Processing Plant Project - Process Description Document No. 82036-02BM-01*, Hanoi.
- Skogestad, S., & Morari, M. (1987). The Dominant Time Constant for Distillation Columns. *Computers & Chemical Engineering*, Vol. 11(6), pp. 607-617, ISSN: 0098-1354.
- Waller, V. (1992). *Practical Distillation Control*, Van Nostrand Reinhold, ISBN: 9780442006013, New York.

Wanren, L.; Julian, C. & Peter, H. (2005). Unit Operations of Chemical Engineering, McGraw-Hill, ISBN : 978-0072848236, New York.

Wuithier, P. (1972). Le Petrole Raffinage et Genie Chimique, Publications de l'Institut Francais du Petrole, ISBN : 978-2710801993, Paris.



Distillation - Advances from Modeling to Applications

Edited by Dr. Sina Zereshki

ISBN 978-953-51-0428-5

Hard cover, 282 pages

Publisher InTech

Published online 23, March, 2012

Published in print edition March, 2012

Distillation modeling and several applications mostly in food processing field are discussed under three sections in the present book. The provided modeling chapters aimed both the thermodynamic mathematical fundamentals and the simulation of distillation process. The practical experiences and case studies involve mainly the food and beverage industry and odor and aroma extraction. This book could certainly give the interested researchers in distillation field a useful insight.

How to reference

In order to correctly reference this scholarly work, feel free to copy and paste the following:

Vu Trieu Minh and John Pumwa (2012). Modeling and Control Simulation for a Condensate Distillation Column, *Distillation - Advances from Modeling to Applications*, Dr. Sina Zereshki (Ed.), ISBN: 978-953-51-0428-5, InTech, Available from: <http://www.intechopen.com/books/distillation-advances-from-modeling-to-applications/modeling-and-control-simulation-for-a-condensate-distillation-column>

INTECH

open science | open minds

InTech Europe

University Campus STeP Ri
Slavka Krautzeka 83/A
51000 Rijeka, Croatia
Phone: +385 (51) 770 447
Fax: +385 (51) 686 166
www.intechopen.com

InTech China

Unit 405, Office Block, Hotel Equatorial Shanghai
No.65, Yan An Road (West), Shanghai, 200040, China
中国上海市延安西路65号上海国际贵都大饭店办公楼405单元
Phone: +86-21-62489820
Fax: +86-21-62489821

© 2012 The Author(s). Licensee IntechOpen. This is an open access article distributed under the terms of the [Creative Commons Attribution 3.0 License](#), which permits unrestricted use, distribution, and reproduction in any medium, provided the original work is properly cited.